Absolute Calibration Using Rayleigh Scattering

Bertrand FOUGNIE – Patrice HENRY
CNES

1. Introduction

The top-of-atmosphere (TOA) signal measured by a satellite sensor observing oceanic targets is in large proportion due to scattering of the incident solar irradiance by atmospheric components, especially in the visible. In this spectral range, the molecular scattering, so-called Rayleigh scattering, is the main process contributing to the TOA signal and this contribution can be accurately predicted and computed using surface pressure, knowing the spectral response of the instrument.

Other processes contributing to the TOA signal are aerosol scattering, back scattering by the water body, diffuse reflection by whitecaps, specular (or Fresnel) reflection by the surface, and gaseous absorption. Satellite acquisitions over such oceanic targets can be selected so that the contribution of these secondary processes is minimized. For these acquisitions, the molecular scattering signal may constitute as much as 90% of the TOA signal, for spectral bands from blue to red bands (typically 443 to 670nm). This forms the basis of the calibration method using Rayleigh scattering.

This method, derived from Vermote et al. (1992), was previously explained in Hagolle et al. (1999). The approach is statistical, in the sense that climatology is used for marine reflectance, and that cases too contaminated by aerosols are rejected, i.e. the effect of aerosols require a very small correction. This contrasts with the vicarious radiometric calibration using in-situ measurements, in which the TOA signal is accurately computed using measurements of aerosol optical properties and water-leaving radiance. The advantage of the method using Rayleigh scattering is that the calibration is neither geographically or geo-physically limited, but it is derived from a large set of oceanic sites, from both hemispheres and for a large set of conditions.

2 Selection of Observations

• Geographical selection : The marine contribution represents 10 to 15% of the TOA signal for the blue bands and is consequently an important source of error in attempting to met the 1 or 2% accuracy on the TOA signal. A climatological study, based on analyzing SeaWiFS data, was performed by Fougnie et al. (2002) to select adequate oceanic sites for which spatial homogeneity is guaranteed and for which moderate seasonal effects exist. Using such pre-defined oceanic sites the dispersion of the results inside a given site is reduced significantly, as well as biases between results obtained over the different sites. In practice, six major oceanic sites were recommended by Fougnie et al. (2002) in the North and South Pacific, the North and South Atlantic, and in the Indian oceans (see Table 1 and Figure 1).

Table 1. Major oceanic sites recommended for the statistical calibration method using Rayleigh scattering. (after Fougnie et al., 2002.)

#	Name	Location	Latitude (deg)		Longitude (deg)	
			min	max	min	max
1	PacSE	South-East of Pacific	-44.9	-20.7	-130.2	-89.0
2	PacNW	North-West of Pacific	10.0	22.7	139.5	165.6
3	PacN	North of Pacific	15.0	23.5	179.4	200.6
4	AtlN	North of Atlantic	17.0	27.0	-62.5	-44.2
5	AtlS	South of Atlantic	-19.9	-9.9	-32.3	-11.0
6	IndS	South of Indian	-29.9	-21.2	89.5	100.1

• Clear-pixel selection : It is obvious that a cloud mask is applied on data, but in addition, only pixels distant by about 10 pixels from a cloud are kept. Furthermore, a strict threshold is applied to the TOA reflectance (in fact the product of reflectance and $\cos(\theta v).\cos(\theta s)$) in order to reject data with sensible aerosol loading and sub-pixel clouds. A threshold is also applied to the surface wind speed extracted from meteorological data to avoid possible contamination by surface whitecaps: only situations with a wind speed smaller than 5m/s are selected. Importantly, we can be very restrictive about these thresholds (only very clear pixels are retained), yet obtain statistically significant results.

• Geometrical selection : Pixels potentially contaminated by sun glint are rejected, i.e. observations with viewing direction inside a cone of ±60° around the specular direction are discarded. Also, acquisitions corresponding to extreme geometries, such as solar or viewing zenith angle greater than 60°, are rejected.

• Ancillary Data : Some exogenous data are necessary to accurately compute the TOA signal, such as the surface pressure, the surface wind speed or the total ozone amount. Naturally, only pixel for which these ancillary data are available are selected.

3 Computation of the TOA signal

The following general formulation is used to compute the TOA signal (reflectance):

$$\rho_{TOA}(\theta_s,\theta_v,\phi) = t_g(\theta_s,\theta_v)\{\rho_A(\theta_s,\theta_v,\phi) + \rho_w(\theta_s,\theta_v,\phi)\ T(\theta_s,\theta_v)\ /[1-S_A.\rho_w(\theta_s,\theta_v,\phi)]\} \quad [1]$$

where θ_s, θ_v, and ϕ are respectively the solar and viewing zenith angles and relative azimuth angle, t_g is the total gaseous transmittance, ρ_A is the molecular and aerosol contribution including coupling terms and specular reflection by the wavy surface, ρ_w is the marine reflectance, T is the total atmospheric transmission for aerosols and molecules and S_A is the atmospheric albedo. Note that t_g depends on the amount of absorbers (essentially ozone), ρ_A on aerosol optical thickness, surface pressure and wind speed, T on surface pressure and wind speed and S_A on aerosol optical thickness. These different terms are evaluated as described below.

• Aerosol and molecular scattering contribution. The atmospheric functions ρ_A, T, and S_A are computed using an accurate radiative transfer model such as the successive order of scattering code of Deuzé et al. (1989). This code includes polarization and specular reflection by the wavy surface. The molecular scattering contribution is accurately computed knowing the surface pressure and the molecular optical thickness corresponding to the considered spectral band. For this, the Rayleigh equivalent optical thickness is calculated for a given spectral band by weighting the spectral optical thickness computed according to Gordon et al. (1988) by the spectral solar irradiance and the spectral response within the band. The background aerosol contribution is computed knowing its optical thickness estimated at 865nm (or another near infrared band) and extrapolated for the considered spectral band using a Maritime 98 aerosol model (Gordon and Wang, 1994). In practice, the restrictive thresholds used for the clear pixel selection lead to a residual aerosol optical thickness lower than 0.05 at 865nm, and usually about 0.02-0.035.

• Marine contribution. This contribution, representing about 10% of the TOA signal, is estimated over the pre-defined oceanic sites through a climatological study (Fougnie et al., 2002). The typical marine reflectance for these sites is 0.033 at 443nm, 0.020 at 490nm, 0.0049 at 555nm, and 0.0007 at 670nm, and is close to values derived through a bio-optical model using a surface pigment concentration of 0.07 m/m^3. A spectral interpolation can be performed when the spectral band of interest is not exactly the same as one of the SeaWiFS spectral bands for which the climalotogical values are available. In addition, a bi-directional correction is added as an option in order to take into account sensible differences in the viewing and solar geometries of the pixel to calibrate and the angular conditions of the climatological values derived from SeaWiFS (e.g. due local time of overpass or case of multidirectional viewing sensors). This correction is made according to Morel et Gentili (1993).

• Gaseous contribution. A gaseous absorption is effected for each spectral band. The main contributors are water vapor (mainly around 565 and 865nm), ozone (mainly around 490, 565, and 670 nm), oxygen

(around 765 nm), nitrogen dioxide (mainly around 443 and 490 nm). The correction is made according to the SMAC model (Rahman and Dedieu, 1994) using exponential variation with air mass and gaseous amount.

4 Error budget

Table 2 summarizes the error budget of the method. For this budget, we have estimated the impact on calibration results of typical uncertainties on the input parameters. We have considered errors made on the surface pressure and surface wind speed (impacting the Rayleigh contribution), on the calibration of the 865nm band and on the expected aerosol model (impacting the aerosol contribution), on the gaseous absorption, and on the marine reflectance. In this error budget evaluation, using the root-mean-squared (RMS) error as a measure of performance is appropriate and realistic, because of the large amount of data considered in the synthesis, i.e. several geometric, geographic, and geophysical conditions.

In general, the error budget, in terms of RMS, is less than 3.5%. For shorter wavelengths, 443, 490, and 510 nm, the performance is determined by the accuracy on the marine reflectance. This confirms the interest of and justifies using in some cases the complementary vicarious approach based on in-situ measurements to improve the accuracy of the statistical results. For wavelengths near 565nm, the performance depends quite equally on the errors of all the parameters. In the red (670nm), error in the calibration in the near infrared (865 nm) becomes the limiting factor to accuracy.

Table 1.2. Typical error budget (in %) for the 6 main sources of uncertainties.

Error (in %)	**443nm**	**490nm**	**510nm**	**565nm**	**670nm**
surface pressure : 10hPa	0.81	0.81	0.81	0.81	0.82
surface wind speed : 2m/s	1.00	1.00	1.00	1.00	1.00
calibration at 865 : 3%	0.50	0.40	0.49	0.74	1.42
aerosol model (50% at 443)	0.57	0.55	0.53	0.42	0.33
gas amount error of 20%	0.12	0.38	0.71	1.62	0.74
marine reflectance	3.06	2.59	2.16	0.96	0.33
RMS	3.41	3.36	3.00	2.43	2.11
MAX	6.06	5.73	5.70	5.55	4.64

5 Calibration algorithm and analysis

The evaluation consists in comparing the TOA normalized radiance computed with the radiative transfer model (Ls) with the normalized radiance derived from the sensor measurements (Lm), assuming a given calibration (the one we want to evaluate). Consequently, the ratio RA_k, defined as Lm/Ls, provides a measure of the discrepancy in calibration coefficients with respect to reference values. This comparison is made for each selected pixel and/or viewing direction. It was evidenced that a site by site analysis is sometimes useful. In fact, residual biases still exist on the knowledge of marine reflectance and these biases differ for each oceanic site. If we limit the analysis to one given site, the bias will be the same for each pixel of the data set, and some particular relative effects (of course not absolute), such as a small temporal decrease or multi-angular calibration errors, become easier to detect.

The analysis with other various parameters can help with understanding potential problems. For example, the variation with viewing geometry (zenith viewing angle for instance) may indicate some problem in the multi-angular calibration. The variation with aerosol content may reveal a problem in the calibration of the 865nm spectral band (or the spectral band used to estimate the aerosol amount) or on

the supposed aerosol model (Maritime 98). The variation with the Rayleigh contribution or with geometry may point to some residual problem with the polarization sensitivity of the instrument.

6 Examples of Application

Figures 2 and 3 display R_{Ak} obtained for POLDER-2 at 443, 490, and 670 nm during the period from January to June 2003 and MERIS at 490 and 620 nm during the period from January to September 2003. The estimated R_{Ak} calibration coefficients for POLDER-2, with respect to pre-launch values, do not depend on aerosol optical thickness, viewing zenith angle, and geographic location for POLDER-2. A small dependence with reflectance is apparent for MERIS, especially at 490 nm, and a small change with time. The values (± one standard deviation) are 0.995 (±0.019), 0.976 (±0.014), and (0.902±0.017) for POLDER-2, and 1.008 (±0.012) and 0.994 (±0.012) for MERIS. The standard deviations represent less than 2% of the R_{Ak} values, attesting of the good accuracy of the method. The temporal evolution of the radiometric calibration may be monitored by systematically and operationally examining suitable sites, allowing not only detection of long-term trends, but also of high frequency changes that may occur as a result of changes in the data processing or due to onboard calibration adjustments, as evidenced in Figure 4 for MERIS.

As the examples illustrate, the Rayleigh scattering method is efficient for the absolute calibration of ocean-color sensors. The method provides calibration coefficients with an inaccuracy of 3-4% (better statistically), for spectral bands in the visible and red. The method is not applicable to the near infrared, where molecular scattering is ineffective. A more accurate specification of the marine reflectance in the blue would reduce uncertainties in this spectral range. Using oligotrophic waters is not ideal in the blue because the marine reflectance is high, but it is difficult to find oceanic areas away from the coast with high and stable chlorophyll concentrations.

7 References

Deuzé, J.-L., M. Herman, and R. Santer, Fourier series expansion of the transfer equation in the atmosphere-ocean system, *J. Quant. Spectrosc. Radiat. Transfer*, **41**, pp. 483-494, 1989.

Gordon, H. R., and M. Wang, Retrieval of water-leaving radiance and aerosol optical thickness over the oceans with SeaWiFS: a preliminary algorithm, *Appl. Opt.*, **33**, pp.443-452, 1994.

Gordon, H. R., J. W. Brown, and R. H. Evans, Exact Rayleigh scattering calculations for use with the Nimbus-7 Coastal Zone Color Scanner, *Appl. Opt.*, **27**, pp. 862-871, 1988.

Morel, A., and B. Gentili, Diffuse reflectance of oceanic waters (2): Bi-directional aspects., *Appl. Opt.*, **32**, pp. 6864-6879, 1993.

Rahman, H., and Dedieu, G. 1994. SMAC: a simplified method for the atmospheric correction of satellite measurements in the solar spectrum. *Int. J. Remote Sensing*, **15**, pp. 123-143.

Fougnie, B., P. Henry, A. Morel, D. Antoine, and F. Montagner, Identification and Characterization of Stable Homogeneous Oceanic Zones : Climatology and Impact on In-flight Calibration of Space Sensor over Rayleigh Scattering, *Proceedings of Ocean Optics XVI*, Santa Fe, New Mexico, 18-22 November, 2002.

Vermote, E., R. Santer, P.-Y. Deschamps, and M. Herman, In-flight calibration of large field of view sensors at shorter wavelengths using Rayleigh scattering*, Int. J. Remote Sensing*, vol. 13, pp. 3409-3429, 1992.

Hagolle, 0., P. Goloub, P.-Y. Deschamps, H. Cosnefroy, X. Briottet, T. Bailleul, J.M.Nicolas, F. Parol, B. Lafrance, and M. Herman, Results of POLDER In-Flight Calibration, *IEEE Trans. on Geosci. Remote Sensing*, vol. 37, pp. 1550-1566, 1999.

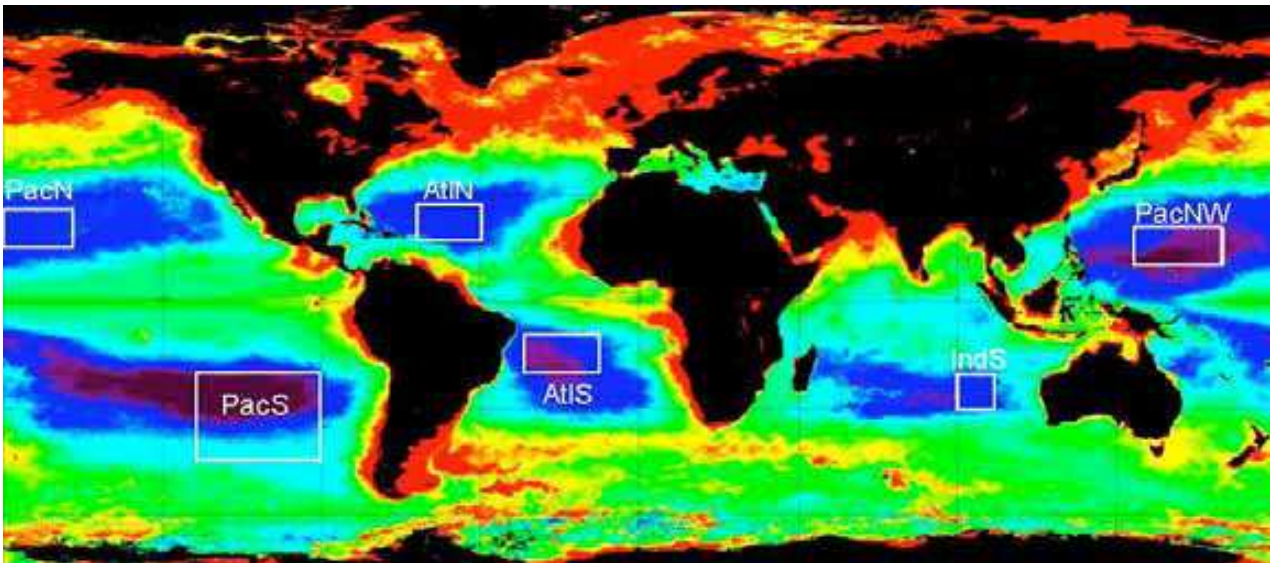

Figure 1. Geographic location of the recommended sites for Rayleigh scattering calibration

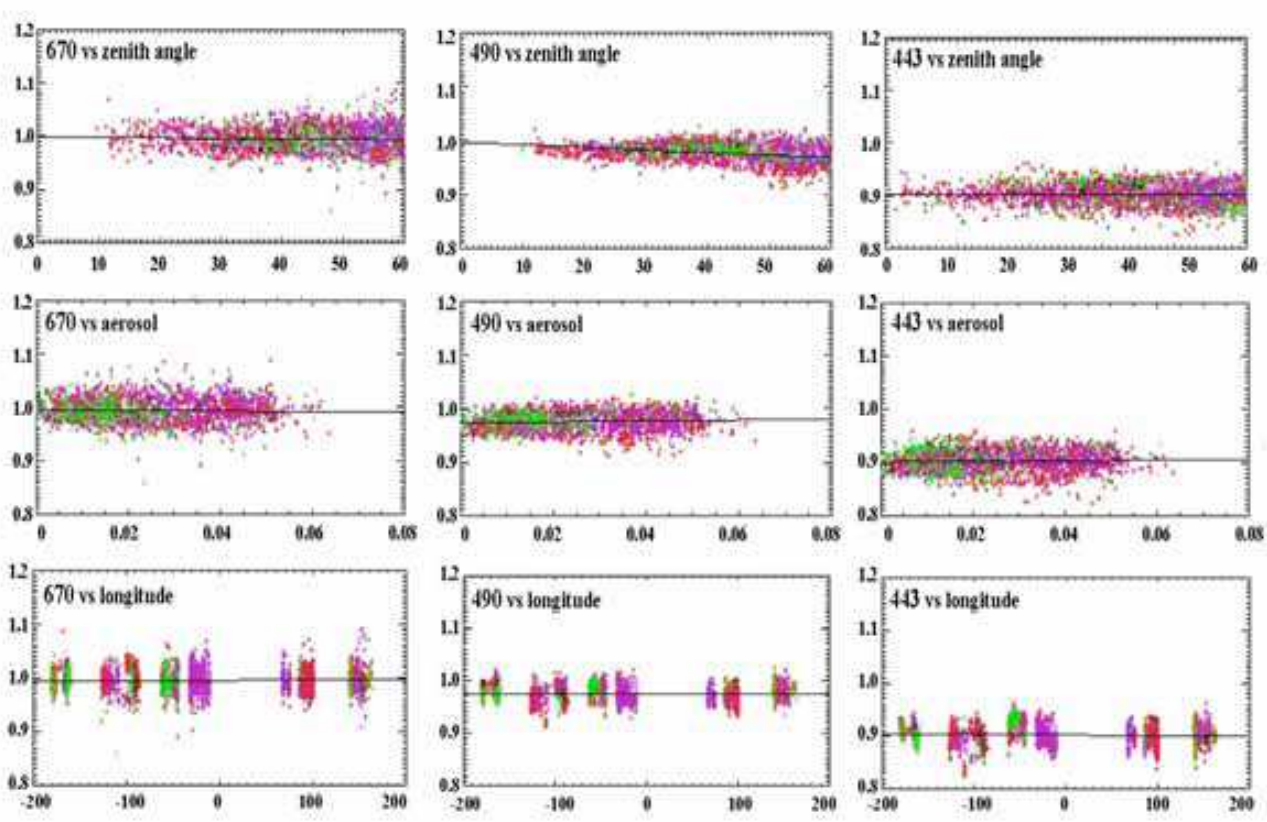

Figure 2. Radiometric calibration of POLDER-2 at 670, 490 and 433 nm (left to right) from January to June 2003. The R*Ak* coefficients are displayed as a function of : viewing zenith angle (top), aerosol optical thickness (middle) and longitude (bottom).

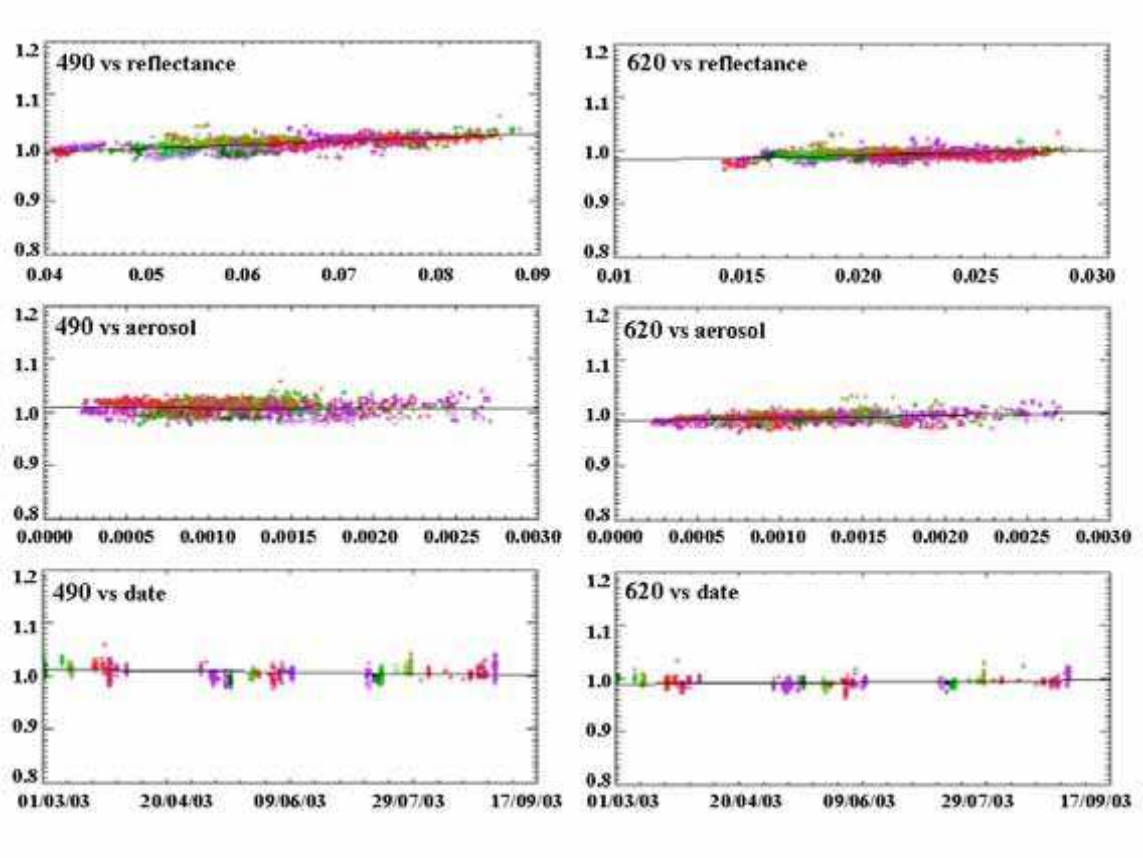

Figure 3. Radiometric calibration of MERIS at 490 nm (left) and 620 nm (right) from January to September 2003. The R*Ak* coefficients are displayed as a function of : measured reflectance (top), aerosol optical thickness (middle), and date (bottom).

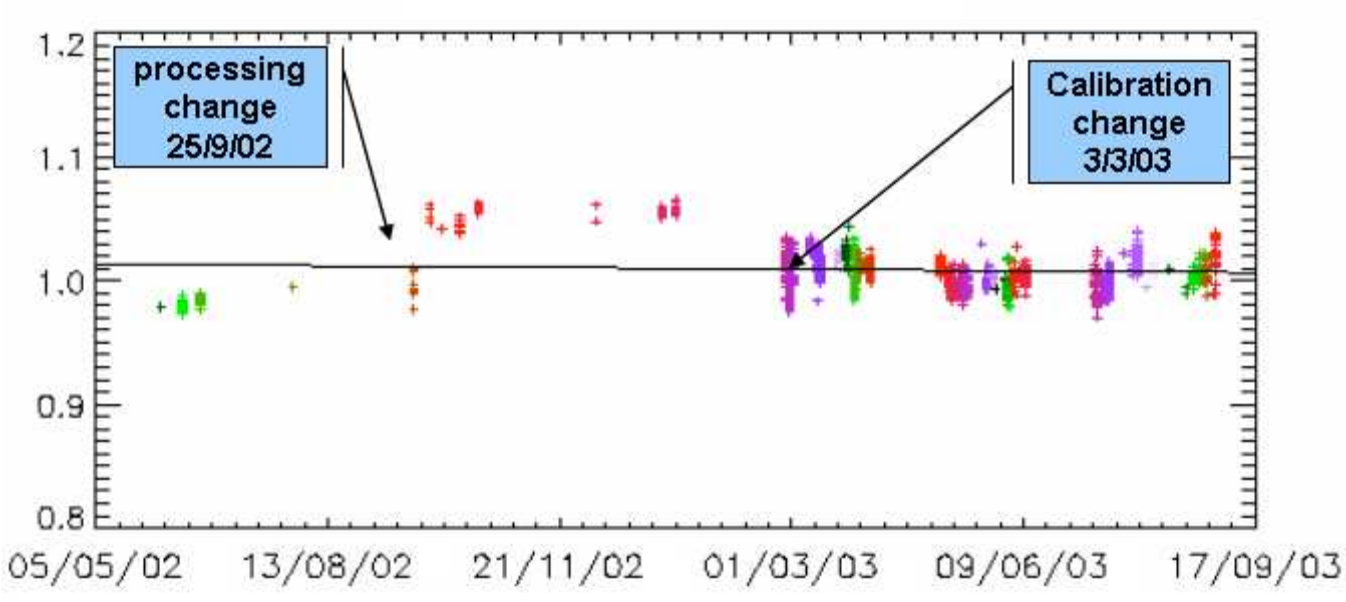

Figure 4. Temporal change in the MERIS calibration coefficient at 490 nm.